JOURNAL OF CHEMICAL INFORMATION AND MODELING

Letter

pubs.acs.org/jcim

Discovery of New Liver X Receptor Agonists by Pharmacophore Modeling and Shape-Based Virtual Screening

Veronika Temml,[†] Constance V. Voss,[‡] Verena M. Dirsch,[‡] and Daniela Schuster*,[†]

[†]Institute of Pharmacy/Pharmaceutical Chemistry and Center for Molecular Biosciences Innsbruck, University of Innsbruck, Innrain 80-82, 6020 Innsbruck, Austria

[‡]Department of Pharmacognosy, Molecular Targets Group, University of Vienna, Althanstr. 14, 1090 Vienna, Austria

Supporting Information

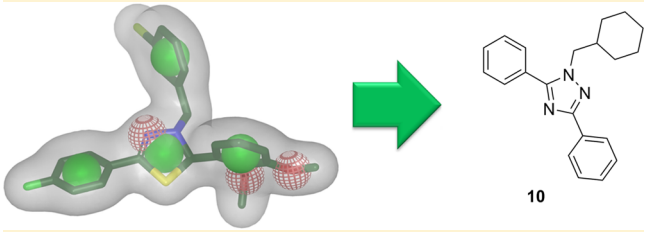

ABSTRACT: Agonists of liver X receptors (LXR) α and β are important regulators of cholesterol metabolism, but agonism of the LXRα subtype appears to cause hepatic lipogenesis, suggesting LXRβ-selective activators are attractive new lipid lowering drugs. In this work, pharmacophore modeling and shape-based virtual screening were combined to predict new LXRβ-selective ligands. Out of the 10 predicted compounds, three displayed significant LXR activity. Two activated both LXR subtypes. The third compound activated LXRβ 1.8-fold over LXRα.

Hypercholesterolemia, dyslipoproteinemia, and inflammation are major risk factors for the development of atherosclerosis and coronary heart disease. Numerous studies have demonstrated that lowering excess plasma cholesterol levels, mainly by reducing low-density lipoprotein (LDL) cholesterol while increasing high density lipoprotein (HDL) cholesterol, helps to slow down the progression of atherosclerosis.[1−3] As a result, there is growing interest in therapeutically targeting reverse cholesterol transport (RCT), the process of cholesterol delivery from peripheral cells to the liver for subsequent elimination.[4−6]

The liver X receptors (LXRα and LXRβ) belong to the nuclear receptor superfamily and are key regulators of cholesterol homeostasis and RCT.[7−9] LXRα is highly expressed in metabolically active tissues, such as liver, intestine, adipose tissue, and macrophages, whereas LXRβ is ubiquitously expressed. Both subtypes share 77% sequence homology in their DNA binding and ligand binding domain. Activated by endogenous oxysterol ligands as well as by several synthetic ligands,[10] LXRs increase reverse cholesterol efflux from cells, including macrophages of atherosclerotic lesion sites, via ATP-binding cassette transporters A1 and G1 (ABCA1 and ABCG1). Extracellular cholesterol is transported to the liver by cholesterol acceptors, such as HDL and lipid-poor apolipoproteins, and converted to bile acids for secretion into bile and its elimination into feces. In addition to the receptors regulatory role in cholesterol metabolism, LXRs also possess anti-inflammatory properties.[11,12] The antiatherosclerotic effect of LXR activation has been demonstrated in numerous studies of murine atherosclerosis models. Treatment of atherosclerotic mice with an LXR agonist reduces disease development, while the loss of LXR expression results in accelerated atherosclerosis.[10,13,14] Despite the antiatherosclerotic properties of LXR agonists, their use as therapeutic agents has been hampered by unfavorable side effects of LXR stimulation, such as increased hepatic lipogenesis, hypertriglyceridemia and liver steatosis.[15,16] These adverse effects are attributed to LXRα, which is the predominant LXR subtype in the liver inducing the expression of genes involved in fatty acid and triglyceride synthesis.[17,18] Hence, it has been proposed that specific targeting of LXRβ may retain antiatherosclerotic benefits, while avoiding hepatic lipogenesis and the development of steatosis.

However, given the degree of structural similarity of the two LXR isoforms, combined with the high flexibility of the binding pocket, subtype-selective agonists may be difficult to attain. Nevertheless, Molteni et al. recently discovered a series of N-acylthiadiazolines subtrates with selectivity for LXRβ.[19]

The aim of this study was to apply a virtual screening workflow to retrieve LXRβ-selective compounds from a 3D compound database. In vitro evaluation of these compounds employing a cell-based LXRα/β-selective luciferase assay should reveal novel LXR ligands with the desired selectivity.

In a previously published study, a set of six structure-based pharmacophore models for LXR agonists was developed.[20] The models were experimentally validated by biological confirmation of the activity of 18 synthetic LXR agonists they had predicted. Four of these virtual hits were active in an assay that determined the relative induction of the LXR-driven luciferase reporter gene ABCA1, but they were not tested on subtype specificity.

To determine whether the available six models had the ability to find the LXRβ-selective scaffold proposed by Molteni et al.,[19] a testset of 14 compounds was assembled and sorted by LXR subtype selectivity (Supporting Information). From these 14 compounds, a 3D multiconformational library was calculated in Discovery Studio[21] using BEST (flexible) settings and a maximum of 100 conformers per molecule. This library was screened against the six pharmacophore models using BEST settings, which allow for a modest conformational ligand

dx.doi.org/10.1021/ci400682b | J. Chem. Inf. Model. XXXX, XXX, XXX−XXX

change during the screening optimizing its fitting into the model. Two models were not able to find any compounds from the data set and were discarded. One model found just one moderately selective structure and was also discarded. The three models 1pqc, 1pq6, and 3fal (Figure 1) found a significant number of highly selective compounds and were therefore selected for the prospective virtual screening for novel LXRβ-selective ligands. Detailed results on these virtual screening experiments and hit lists are available in the Supporting Information.

To additionally increase the chance of finding a LXRβ-selective hit, a shape-based rapid overlay of chemical structures (ROCS)[23] screening was performed.[24] The most selective agonist from the Molteni series (compound **1**, $EC_{50(LXR\beta)}$ = 0.25 μM, not active on LXR-α) was used as a ROCS shape query (Figure 2). In this method, a low energy 3D conformer of a compound is calculated, and a shape is derived from the molecule's surface. This query shape is then compared to the shapes of compounds in a 3D database during the screening process. Molecules fitting the query shape are expected to be most likely active on the target. The overlap of two molecules is estimated with Gaussians parametrized according to the volume of the occurring heavy atoms. In addition, complementary properties in chemical functionalities are calculated. Both, overlap in shape and chemical functionality are quantified in ROCS's ComboScore (CS), which combines the shape Tanimoto and scaled color score. Both of these range from 0 to 1 so the CS ranges from 0 to 2, with 2 representing maximal similarity (identity).

The shape query was set to screen the Specs virtual library,[28] containing 202,879 entries. A 3D database of maximal 400 conformers per molecule was calculated from the SPECS database using OMEGA[25−27] with standard settings. The ROCS search reported the best-ranked 500 compounds, of which 160 had a CS above 1.3. To narrow down the number of virtual hits, the three selective pharmacophore models (Figure 1) were used for filtering the hits. A Discovery Studio 3D conformational database was generated and screened using the same settings as before for the 14 LXRβ agonists.[19] This search found 56 compounds among the 500 hits from the ROCS screening.

Out of all the hits, 10 compounds (Chart 1) were selected for biological testing. The hits were primarily selected according to the CS assigned by the ROCS software. In addition, hits that were additionally found by the pharmacophore models were favored. Nine of the selected compounds had a high CS of more than 1.3. The tenth selected hit had a CS of 1.27; however, it was found by three pharmacophore models and therefore was additionally selected for biological evaluation. Compounds that were already known to have LXR activity or to be unstable under biological conditions could not be attained with over 90% purity or were too similar to already selected compounds were discarded.

Finally, the selected 10 hits were evaluated in an LXR luciferase reporter gene assay. In general, this assay is used to measure the transactivation activity of LXR via respective ligands. The LXR reporter plasmid (hLXREx3TK-Luc) contains a luciferase reporter gene under the control of a promotor including three copies of an LXR response element. Upon ligand binding, the LXR receptor translocates to the nucleus, where it binds to the LXR response elements in the reporter plasmid hLXREx3TK-Luc. An agonistic activity of the LXR ligand leads to the expression of the luciferase reporter gene. The measured activity of expressed luciferase provides a measure for the transactivation activity of the respective LXR ligand.

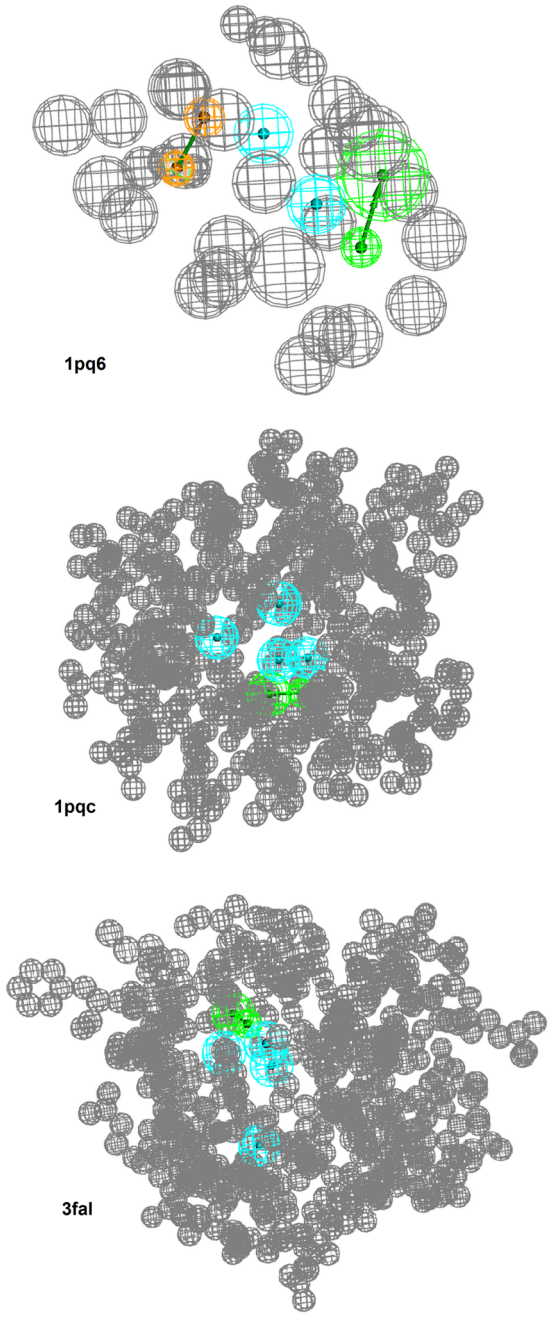

Figure 1. Pharmacophore models that showed a significant enrichment of highly LXRβ-selective compounds. The models are named after the X-ray crystal structure protein data bank[22] code from which they were originally derived. Blue spheres illustrate hydrophobic features. Green arrows represent hydrogen bond acceptors. Brown spheres represent aromatic interactions with indicated direction. The gray spheres signify so-called exclusion volumes that represent the space occupied by the protein. Model 1pc6 consists of two hydrophobic features, one hydrogen bond acceptor, an aromatic interaction, and 31 exclusion volumes. Model 1pqc consists of three hydrophobic features, one hydrogen bond acceptor, and 458 exclusion volumes. Model 3fal consists of three hydrophobic features, one hydrogen bond acceptor, and 514 exclusion volumes.

dx.doi.org/10.1021/ci400682b | J. Chem. Inf. Model. XXXX, XXX, XXX−XXX

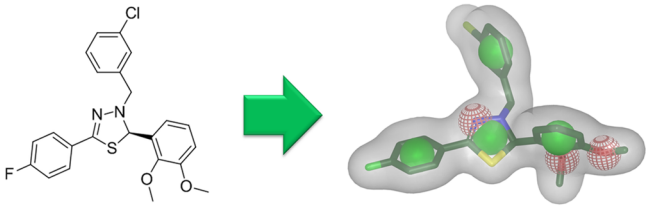

Figure 2. ROCS shape query derived from a low energy 3D conformation generated in Omega[25] of the LXRβ-selective ligand **1**.The green spheres illustrate ROCS ring features, and the red spheres illustrate hydrogen bond acceptors.

In detail, for the LXR luciferase reporter gene assay, HEK293 cells were cultured in tissue culture flasks in phenol red-free DMEM medium supplemented with 10% FBS, 1% glutamine, and 1% penicillin/streptomycin in an incubator at 37 °C and 5% CO_2. One day before the transfection experiment, cells were trypsinized and plated into a 96-well plate at a density of 40.000 cells/well. The next day, at a cell confluency of >80%, the medium was replaced by antibiotic-free DMEM supplemented with 5% FBS and 1% glutamine. Cells were transiently transfected with hLXREx3TK-Luc as a reporter plasmid (0.05 μg/well), pCMV-hLXR-α or pCMV-hLXR-β as expression vectors (each 0.025 μg/well), and GFP (0.025 μg/well) as internal transfection control according to the manufactures protocol (FuGene HD, Roche). After 24 h incubation with the transfection mixture, the medium was replaced by phenol red-free DMEM including 10% charcoal stripped FBS, and the cells were treated with the compounds **2**−**11** at indicated concentrations. LXR agonist GW3965 (Sigma-Aldrich) was used as the positive control and DMSO as the negative control. At the end of the incubation period, the cells were lysed and assayed for luciferase activity using a Tecan GENios Pro plate-reading luminometer.

The cell-based LXRα- or LXRβ-selective reporter gene assay revealed LXR binding activity for three out of 10 tested compounds (Figure 3). At a concentration of 10 μM, compound **10** showed the highest LXR activity but no LXR subtype selectivity. Moderately active compound **8** also exhibited no selectivity for LXRβ. However, compound **3** showed an almost 2-fold higher activation (selectivity factor: LXRβ/LXRα = 1.8) of LXRβ compared to LXRα.

Compared to the full LXR agonist GW3965, compounds **3**, **8**, and **10** are moderately but significantly active. Because the full LXR agonists show several adverse side effects in regard to increased hepatic lipogenesis, the moderate or partial LXR activation of compounds **3**, **8**, and **10** might be advantageous.

In summary, out of nine compounds selected by the ROCS shape-based screening with a CS above 1.3, three active compounds were found (**3**, **8**, and **10**), one of them displaying LXRβ selectivity (compound **3**). Two of them had also been predicted as active by the pharmacophore models (**3** and **8**). The LXRβ-selective active compound **3** was found by the models 1pq6 and 1pqc, while compound **8** was found by 1pqc alone. These two validated pharmacophore models can be employed for future screening studies.

It should be emphasized that it was the combination of both methods that enabled us to find all the active compounds. If only pharmacophore-based screening would have been used, the highly active compound **10** would have been missed. On the other hand, the only LXRβ selective compound **3**, which barely made the CS cutoff, was primarily selected because it was also predicted to be active by two pharmacophore models.

Chart 1. 10 Virtual Hits Selected for Biological Testing[a]

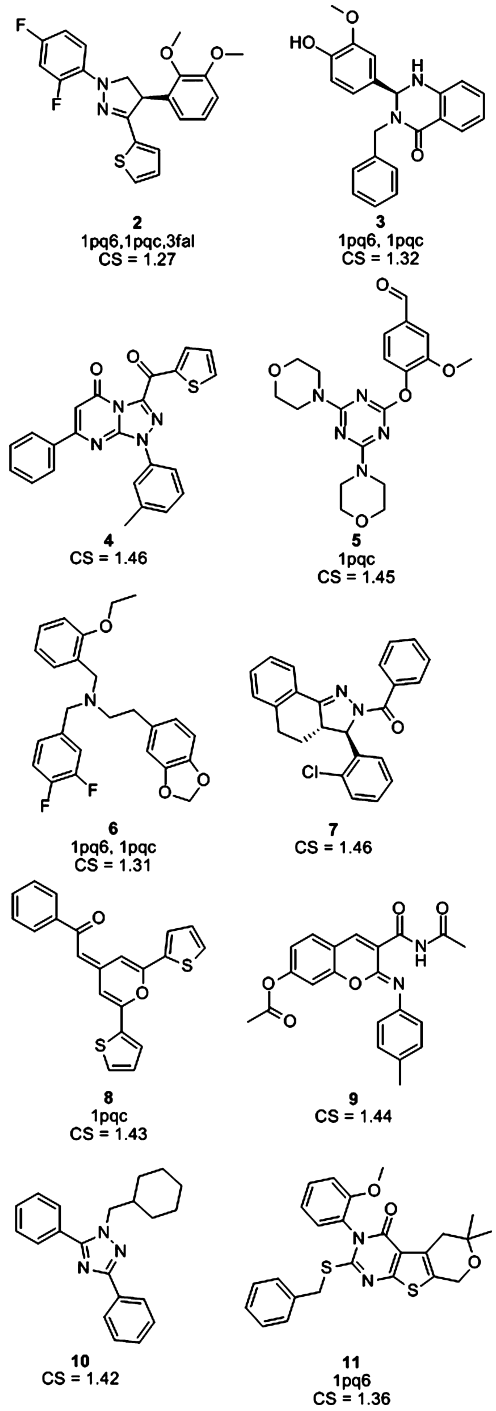

[a]The fitting pharmacophore models and CS are indicated for every structure.

This study provides a promising computational approach for further investigations on the prediction of LXRβ selective ligands with pharmacophore modeling and shape-based virtual screening. Derivatives of **3** and **10** could be synthesized to obtain a clearer idea of the structure−activity relationship required for compounds with LXRβ selectivity.

Because of the pronounced activity of **10**, a more thorough characterization of its activity on cells and in vivo is in progress.

dx.doi.org/10.1021/ci400682b | J. Chem. Inf. Model. XXXX, XXX, XXX−XXX

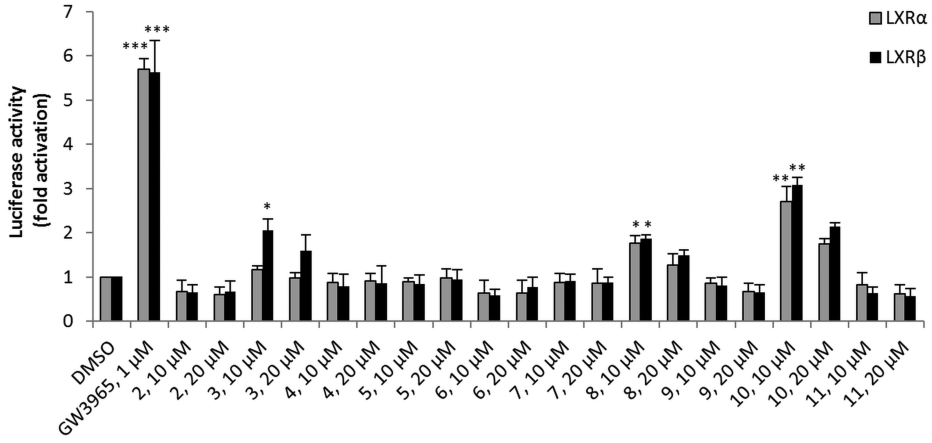

Figure 3. Effect of compounds **2**–**11** and LXR agonist GW3965 on LXRα- and LXRβ-luciferase activity in HEK293 cells. HEK293 cells were transiently transfected with hLXREx3TK-Luc as a reporter plasmid, pCMV-hLXR-α or pCMV-hLXR-β as expression vectors, and GFP as internal transfection control. Cells were treated with the indicated compounds. LXR agonist GW3965 was used as the positive control and DMSO as the negative control. At the end of the incubation period, the cells were lysed and assayed for luciferase activities. The results are expressed as relative luciferase activity (fold difference compared to solvent control). All values are means ± SEM (n = 3, each in quadruplicate) vs control, *p < 0.05, **p < 0.01, and ***p < 0.001.

■ ASSOCIATED CONTENT

Supporting Information

Pharmacophore-based screening results of the 14 LXR ligands from Molteni et al.[19] This material is available free of charge via the Internet at http://pubs.acs.org.

■ AUTHOR INFORMATION

Corresponding Author

*Tel: +43 512 507 58253. Fax: +43 512 507 58299. E-mail: daniela.schuster@uibk.ac.at.

Author Contributions

The study was initiated and designed by all authors. V.T. and D.S. conducted the computational study. C.V.V. and V.M.D. performed the in vitro LXR tests. The manuscript was written through contributions of all authors. All authors have given approval to the final version of the manuscript.

Notes

The authors declare no competing financial interest.

■ ACKNOWLEDGMENTS

The LXR reporter gene plasmid was kindly provided by Dr. Valery Bochkov, University of Vienna. This study was financed by the Austrian Science Fund (FWF): S10704 and S10711 (national research network (NFN) "Drugs from Nature Targeting Inflammation"). D.S. is supported by the Erika Cremer Habilitation Program and a Young Talents Grant of the University of Innsbruck. We thank Inte:Ligand and OpenEye for providing LigandScout, OMEGA and ROCS free of charge.

■ ABBREVIATIONS

ABCA1, ATP-binding cassette transporters A1; ABCG1, ATP-binding cassette transporters G1; CS, ROCS ComboScore; DMSO, dimethyl sulfoxide; GFP, green fluorescent protein; HDL, high density lipoprotein; HEK293, human embryonic kidney 293 cells; LXR, liver X receptor; RCT, reverse cholesterol transport; ROCS, rapid overlay of chemical structures

■ REFERENCES

(1) Ibanez, B.; Vilahur, G.; Cimmino, G.; Speidl, W. S.; Pinero, A.; Choi, B. G.; Zafar, M. U.; Santos-Gallego, C. G.; Krause, B.; Badimon, L.; Fuster, V.; Badimon, J. J. Rapid change in plaque size, composition, and molecular footprint after recombinant apolipoprotein A-I Milano (ETC-216) administration: Magnetic resonance imaging study in an experimental model of atherosclerosis. *J. Am. Coll. Cardiol.* **2008**, *51*, 1104–1109.

(2) Nissen, S. E.; Tsunoda, T.; Tuzcu, E. M.; Schoenhagen, P.; Cooper, C. J.; Yasin, M.; Eaton, G. M.; Lauer, M. A.; Sheldon, W. S.; Grines, C. L.; Halpern, S.; Crowe, T.; Blankenship, J. C.; Kerensky, R. Effect of recombinant ApoA-I Milano on coronary atherosclerosis in patients with acute coronary syndromes: A randomized controlled trial. *JAMA, J. Am. Med. Assoc.* **2003**, *290*, 2292–2300.

(3) Tardif, J.-C.; Grégoire, J.; L'Allier, P. L.; Ibrahim, R.; Lespérance, J.; Heinonen, T. M.; Kouz, S.; Berry, C.; Basser, R.; Lavoie, M.-A.; Guertin, M.-C.; Rodés-Cabau, J. Effects of reconstituted high-density lipoprotein infusions on coronary atherosclerosis: A randomized controlled trial. *JAMA, J. Am. Med. Assoc.* **2007**, *297*, 1675–1682.

(4) Cuchel, M.; Rader, D. J. Macrophage reverse cholesterol transport: Key to the regression of atherosclerosis? *Circulation* **2006**, *113*, 2548–2555.

(5) Tall, A. R. Cholesterol efflux pathways and other potential mechanisms involved in the athero-protective effect of high density lipoproteins. *J. Intern. Med.* **2008**, *263*, 256–273.

(6) Santos-Gallego, C. G.; Ibanez, B.; Badimon, J. J. HDL-cholesterol: Is it really good? Differences between apoA-I and HDL. *Biochem. Pharmacol.* **2008**, *76*, 443–452.

(7) Beaven, S. W.; Tontonoz, P. Nuclear receptors in lipid metabolism: Targeting the heart of dyslipidemia. *Annu. Rev. Med.* **2006**, *57*, 313–329.

(8) Kalaany, N. Y.; Mangelsdorf, D. J. LXRs and FXR: The yin and yang of cholesterol and fat metabolism. *Annu. Rev. Med.* **2006**, *68*, 159–191.

(9) Calkin, A. C.; Tontonoz, P. Transcriptional integration of metabolism by the nuclear sterol-activated receptors LXR and FXR. *Nat. Rev. Mol. Cell. Biol.* **2012**, *13*, 213–224.

(10) Jakobsson, T.; Treuter, E.; Gustafsson, J.-A.; Steffensen, K. R. Liver X receptor biology and pharmacology: new pathways, challenges and opportunities. *Trends Pharmacol. Sci.* **2012**, *33*, 394–404.

(11) Joseph, S. B.; Castrillo, A.; Laffitte, B. A.; Mangelsdorf, D. J.; Tontonoz, P. Reciprocal regulation of inflammation and lipid metabolism by liver X receptors. *Nat. Med.* **2003**, *9*, 213–219.

(12) Zelcer, N.; Tontonoz, P. Liver X receptors as integrators of metabolic and inflammatory signaling. *J. Clin. Invest.* **2006**, *116*, 607−614.
(13) Tangirala, R. K.; Bischoff, E. D.; Joseph, S. B.; Wagner, B. L.; Walczak, R.; Laffitte, B. A.; Daige, C. L.; Thomas, D.; Heyman, R. A.; Mangelsdorf, D. J.; Wang, X.; Lusis, A. J.; Tontonoz, P.; Schulman, I. G. Identification of macrophage liver X receptors as inhibitors of atherosclerosis. *Proc. Natl. Acad. Sci. U. S. A.* **2002**, *99*, 11896−11901.
(14) Joseph, S. B.; McKilligin, E.; Pei, L.; Watson, M. A.; Collins, A. R.; Laffitte, B. A.; Chen, M.; Noh, G.; Goodman, J.; Hagger, G. N.; Tran, J.; Tippin, T. K.; Wang, X.; Lusis, A. J.; Hsueh, W. A.; Law, R. E.; Collins, J. L.; Willson, T. M.; Tontonoz, P. Synthetic LXR ligand inhibits the development of atherosclerosis in mice. *Proc. Natl. Acad. Sci. U.S.A.* **2002**, *99*, 7604−7609.
(15) Repa, J. J.; Liang, G.; Ou, J.; Bashmakov, Y.; Lobaccaro, J.-M. A.; Shimomura, I.; Shan, B.; Brown, M. S.; Goldstein, J. L.; Mangelsdorf, D. J. Regulation of mouse sterol regulatory element-binding protein-1c gene (SREBP-1c) by oxysterol receptors, LXRa and LXRb. *Genes Dev.* **2000**, *14*, 2819−2830.
(16) Yoshikawa, T.; Shimano, H.; Amemiya-Kudo, M.; Yahagi, N.; Hasty, A. H.; Matsuzaka, T.; Okazaki, H.; Tamura, Y.; Iizuka, Y.; Ohashi, K.; Osuga, J.-I.; Harada, K.; Gotoda, T.; Kimura, S.; Ishibashi, S.; Yamada, N. Identification of liver X receptor-retinoid X receptor as an activator of the sterol regulatory element-binding protein 1c gene promoter. *Moll. Cell. Biol.* **2001**, *21*, 2991−3000.
(17) Lehrke, M.; Lebherz, C.; Millington, S. C.; Guan, H.-P.; Millar, J.; Rader, D. J.; Wilson, J. M.; Lazar, M. A. Diet-dependent cardiovascular lipid metabolism controlled by hepatic LXRa. *Cell Metab* **2005**, *1*, 297−308.
(18) Bradley, M. N.; Hong, C.; Chen, M.; Joseph, S. B.; Wilpitz, D. C.; Wang, X.; Lusis, A. J.; Collins, A. R.; Hsueh, W. A.; Collins, J. L.; Tangirala, R. K.; Tontonoz, P. Ligand activation of LXRb reverses atherosclerosis and cellular cholesterol overload in mice lacking LXRa and apoE. *J. Clin. Invest.* **2007**, *117*, 2337−2346.
(19) Molteni, V.; Li, X.; Nabakka, J.; Liang, F.; Wityak, J.; Koder, A.; Vargas, L.; Romeo, R.; Mitro, N.; Mak, P. A.; Seidel, H. M.; Haslam, J. A.; Chow, D.; Tuntland, T.; Spalding, T. A.; Brock, A.; Bradley, M. N.; Castrillo, A.; Tontonoz, P.; Saez, E. N-Acylthiadiazolines, a new class of liver X receptor agonists with selectivity for LXRb. *J. Med. Chem.* **2007**, *50*, 4255−4259.
(20) von Grafenstein, S.; Mihály-Bison, J.; Wolber, G.; Bochkov, V. N.; Liedl, K. R.; Schuster, D. Identification of novel liver X receptor activators by structure-based modeling. *J. Chem. Inf. Model.* **2012**, *52*, 1391−1400.
(21) Discovery Studio, version 3.0; Accelrys: San Diego, CA; 2012. www.accelrys.com.
(22) Berman, H. M.; Westbrook, J.; Feng, Z.; Gililand, G.; Bhat, T. N.; Weissig, H.; Shindyalov, I. N.; Bourne, P. E. The protein data bank. *Nucleic Acids Res.* **2000**, *28*, 235−242.
(23) ROCS, version 2.3.1.; OpenEye Scientific Software: Santa Fe, NM, 2013. www.eyesopen.com.
(24) Grant, J. A.; Gallardo, M. A.; Pickup, B. T. A fast method of molecular shape comparison: A simple application of a Gaussian description of molecular shape. *J. Comput. Chem.* **1996**, *17*, 1653−1666.
(25) OMEGA, 2.2.1.; OpenEye Scientific Software Inc.: Santa Fe, NM, 2013, www.eyesopen.com.
(26) Hawkins, P. C. D.; Skillman, A. G.; Warren, G. L.; Ellingson, B. A.; Stahl, M. T. Conformer Generation with OMEGA: Algorithm and Validation Using High Quality Structures from the Protein Databank and Cambridge Structural Database. *J. Chem. Inf. Model.* **2010**, *50*, 572−584.
(27) Hawkins, P. C. D.; Nicholls, A. Conformer Generation with OMEGA: Learning from the Data Set and the Analysis of Failures. *J. Chem. Inf. Model.* **2012**, *52*, 2919−2936.
(28) Specs compound library, 2012. www.specs.net.